euronoise

The variability of acoustical turbulence in the atmospheric boundary layer

Sylvain Cheinet

ISL, 5 Rue du General Cassagnou, BP 70034, 68301 Saint-Louis, France
sylvain.cheinet@isl.eu

Outdoor sound propagation is affected by small-scale turbulence, quantified through the refractive index structure parameter C_n^2. In this study, a Large Eddy Simulation (LES) is used to reveal the spatial and temporal variability of C_n^2 in the atmospheric convective boundary layer. A considerable variability is predicted, of almost two orders of magnitude at all heights. The regions of high C_n^2 match the convective plumes that drive the boundary layer dynamics. The impact of this variability on line-of-sight propagation and on sound scattering is illustrated. It is found to result in fluctuations of the considered acoustical diagnostics, which can in some cases induce major changes in the estimation of sensing performances.

1 Introduction

It is well-recognized that the refractive effects perturb a propagating signal in the atmosphere. Physically, the spatial variations of the atmospheric wind and temperature (denoted u and T) cause some variations of the refractive index *n*. [The impact of humidity is not considered in this study]. In the conventional terminology, refraction relates to well-defined gradients in wind and temperature, usually strongest on the vertical. For example, a near-surface unstable thermal stratification decreases the near-surface sound levels, with the formation of a so-called shadow zone. In the additional presence of a wind gradient, the sound levels further decrease upwind and increase downwind.

Turbulence is another major cause of variations of n, of a more fluctuating nature. In line-of-sight propagation, it alters the signal coherence and angle-of-arrival. Besides, the induced sound scattering can significantly increase the acoustical levels in refractive shadow zones. This process is of primary importance to evaluate the detectability area of a given source. It is also at the basis of the sodar technology.

Whereas turbulence spans over a wide range of eddy scales, many of the effects above relate to atmospheric fluctuations in the inertial-convective range, with typical eddy sizes of 1cm to 1m. The fluctuations of a scalar *s* are then locally quantified through the structure parameter of *s*, denoted C_s^2. Hence, the major results of wave propagation theory through turbulent media write in terms of C_n^2. For example, the sound scattering cross section by a volume located in *x* is given by [1]:

$$\sigma(x;\theta) \propto k^{1/3}\left(\sin\frac{\theta}{2}\right)^{-11/3} C_n^2(x;\theta) \qquad (1)$$

with *k* the wavenumber and θ the scattering angle. Also, in line-of-sight propagation (θ≈0) under the smooth perturbations approximation, the transverse coherence length and scintillation rate of a spherical wave write as:

$$\rho_c = \left(1.46k^2 L^{-5/3}\int_0^L x^{5/3} C_n^2(x)dx\right)^{-3/5} \qquad (2)$$

$$S_A = 0.56k^{7/6}L^{-5/6}\int_0^L \left(x(L-x)\right)^{5/6} C_n^2(x)dx$$

with L the propagation range. S_A measures the relative acoustical pressure fluctuations. ρ_c characterizes the distance over which the wave stays coherent. Specific applications like signal beam-forming critically depend on ρ_c [2].

In the dry atmosphere, n depends on u and T, so C_n^2 directly follows from the temperature and wind structure parameters, C_T^2 and C_u^2. The general relation writes as [3]:

$$C_n^2(\theta) = \frac{1}{4}\left(1-2\sin^2\frac{\theta}{2}\right)^2 \frac{C_T^2}{T_0^2} + \frac{11}{6}\left(\cos^2\frac{\theta}{2}\cos^2\theta\right)\frac{C_u^2}{c_0^2} \qquad (3)$$

with c_0 and T_0 some reference sound celerity and temperature. It is thus of primary interest to document, understand and predict the distribution of C_T^2 and C_u^2 in the atmosphere. Many propagation scenarii lie within the atmospheric boundary layer. There, airplanes, radiosondes or ground platforms sample some aspects of the distribution of the atmospheric structure parameters. Remote sensing techniques may also be of help (scintillometry, radars, sodars), still with a sampling representativeness issue. For this reason, the actual statistical distribution and spatial organization of C_n^2 remains largely undocumented [4].

Numerical simulation offers a complementary alternative to access four-dimensional fields. In the last decades, Large Eddy Simulations (LES) have largely enriched the understanding of the boundary layer dynamics. More recently, they have been used as input atmospheric fields in wave propagation models, in electromagnetism as well as in acoustics. This approach requires a massive computational effort, without gaining from the readily available and well-understood analytical solutions of eq (1,2).

The rationale of the present work is that some insight may be gained on the relevant turbulent scales from the LES physics. Specifically, the variability of C_n^2 in the boundary layer can be documented from the LES fields, without the recourse to high spatial resolution. Provided that eq (1,2) hold, their application then allows to derive the impact of the LES variability on some acoustical propagation diagnostics. The study is composed as follows. Section 2 describes the method used to derive the inertial-convective turbulence parameters in 3D+time from LES. Section 3 analyzes the variability of these structure parameters in a specific weather regime. Section 4 investigates the impact of this variability on acoustical propagation. Section 5 summarizes and discusses the results.

2 Structure parameters in LES

The principle of LES is to solve the atmosphere-governing equations in which eddies of sizes smaller than a truncation size Δ_c, in the inertial-convective range, are filtered. LES of boundary layer turbulence have been satisfactorily evaluated against experimental data, over sea and land, under clear and cloudy conditions. In convective conditions, the dynamics of the simulated eddies mimic that of observations. LES have a documented deficiency in the first few tens of meters. In the context of line-of-sight propagation, this formally hampers the assessment of common ground-to-ground scenarii. On the other hand, there is a growing interest for airborne acoustical sensing (e.g. with aerostats). Besides, the sound scattering may be caused by turbulence at higher levels, especially at large acoustical ranges.

To compute C_T^2 and C_u^2, the method of [5] is used. The starting point is the well-known inertial-convective range scaling, which relates C_T^2 and C_u^2 to the dissipation rates of the sub-grid Turbulent Kinetic Energy (TKE) and temperature variance:

$$C_u^2 \equiv \frac{\alpha_1}{0.25}\,\varepsilon_{TKE}^{2/3} \qquad C_T^2 \equiv \frac{\beta_1}{0.25}\,\varepsilon_T\,\varepsilon_{TKE}^{-1/3} \tag{4}$$

where experiments suggest α_1=0.52 and β_1=0.4. From budget arguments, ε_{TKE} and ε_T are parameterized with:

$$\varepsilon_{TKE} = \mathrm{A}_u \frac{TKE^{3/2}}{\Delta_c} \qquad \varepsilon_T = N_s \Delta_c \sqrt{TKE}\left(\frac{\partial T_{pot}}{\partial x_i}\right)^2 \tag{5}$$

with summation over i=1,3. The potential temperature T_{pot} replaces T to account for pressure relaxation. The constants A_u and N_s write in terms of α_1, β_1 and the Prandtl number Pr. C_u^2 and C_T^2 finally take the form:

$$C_u^2 \propto TKE\,\Delta_c^{-2/3} \qquad C_T^2 \propto \frac{1}{\mathrm{Pr}}\frac{\beta_{1,loc}}{\alpha_{1,loc}}\Delta_c^{4/3}\left(\frac{\partial T_{pot}}{\partial x_i}\right)^2 \tag{6}$$

The LES considered hereafter uses Pr=0.33 and in most cases Δ_c=2.5Δ, with Δ the LES spatial resolution [5]. It has cyclic lateral boundary conditions, a damping layer at the top, and prescribed surface fluxes at the bottom. T_{pot} and TKE are available from the LES, and the gradients in eq (5,6) are approximated with finite-differences.

3 Analysis of a case study

This study focuses on the specific weather regime of a purely convective boundary layer, with no clouds and no mean wind. The initial potential temperature lapse rate is of 3K.km^{-1}. The turbulence is driven by the prescribed surface fluxes of sensible heat (0.1Km.s^{-1}) and momentum (-0.073m^2.s^{-2}). This set-up is representative of fair weather regimes with calm winds, over land in the daytime or over warm oceans. The LES domain is 10km*10km*2km, and the run lasts 10000 s. The model has 256*256*64 grid points, with a resolution of 39m on the horizontal and 32m on the vertical. A time-step of 1s is used.

The mean and turbulence structure in the present LES simulation are already discussed in [5]. Some relevant results are here briefly summarized. The predicted flow rapidly reaches a quasi-steady state, with the expected formation of a well-mixed boundary layer, capped by a temperature inversion. At t=10000s the mixed layer height is Zi=1000m. The mean profiles of ε_{TKE} and ε_T match the theoretical expectations, namely, the mean profile ε_{TKE} is almost constant with height and the mean ε_T decreases as $z^{-4/3}$ with z the height. The LES tends to underestimate these quantities compared to observations. A comparable feature apparently arises with other LES. It may be caused by an alteration of the resolved fields at small separations by the sub-grid scales.

The major advance of LES is to provide a new insight on the variability of C_u^2 and C_T^2. Fig 1 shows the probability density function (pdf) with height of the Log of these variables. According to the LES, C_u^2 and C_T^2 vary by almost two orders of magnitude at all levels, a variability that is even greater for C_T^2 than for C_u^2. A further analysis of the LES predictions suggests that the log-normal distribution is a first-order model of the pdf of C_u^2 and C_T^2 at all heights (see also fig 4).

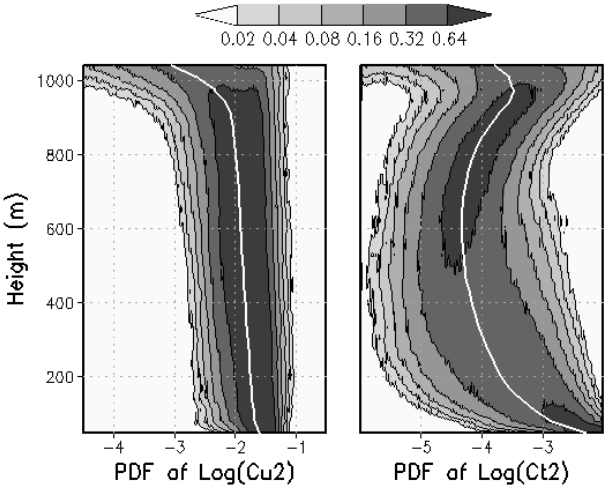

Fig 1: pdf of (left) Log (C_u^2) and (right) Log (C_T^2) with height, with average values as white line.

In the considered case, $C_n^2(\theta=0)$ is dominated by the temperature fluctuations in the surface layer, and by wind fluctuations in the bulk and upper boundary layer. According to similarity laws, the transitional height increases with the surface flux. Surface fluxes can be much larger than the value selected in this study, so the transitional height is likely to reach the bulk boundary layer in some cases.

4 Impact on propagation

A common practice in wave propagation studies is to characterize turbulence in the wave propagation environment with the mean profile of C_n^2. The considerable variability of C_u^2 and C_T^2 indeed challenges this view. This section illustrates the impact of this variability on some acoustical propagation diagnostics. In lines with the non-deterministic character of LES predictions, focus is put on the statistical distribution of these diagnostics.

4.1 Line-of-sight propagation

The (transverse) wave coherence length and scintillation rate are first investigated. To that purpose, the following propagation scenarii are built: a source located at various heights emits at an acoustical frequency of 500Hz. The considered propagation path is horizontal, with a range of L=2km. The LES provides more than fifty grid points along the path, which guarantees a satisfactory discretization of the path integration in eq (2). In order to reach statistical representativeness, the analysis combines a temporal sampling (every 20s over 10 times) with a spatial sampling (252 paths along the x-axis, the propagation path is the y-axis).

Fig 2 shows the pdf of the scintillation rate and the wave coherence length, as obtained from the numerical integration of eq (2) with the LES predictions of C_n^2. The wave coherence length is larger than $\sqrt{\lambda L}$, the size of the most efficient eddies that perturb the initial wave. Accordingly, the smooth perturbations assumption is valid, as the scintillation rate is lower than 0.1. The predicted coherence lengths are one order of magnitude greater than

those reported in [2]. This difference is likely to stem from the much higher turbulence rate in their near-surface experiment. The present result gives a hint that it may be feasible to beam-form a signal sensed from an aerostat, at least in some circumstances.

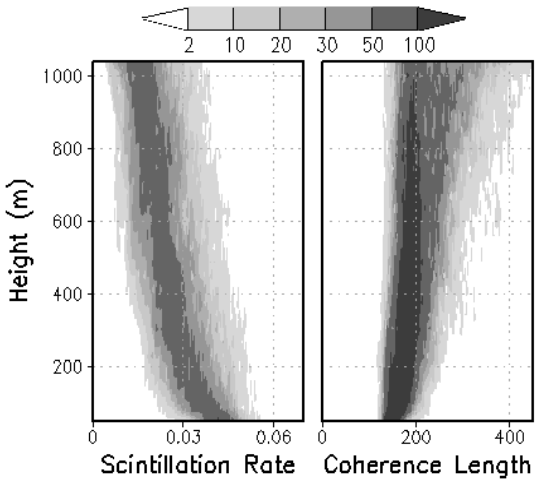

Fig 2: pdf with height of (left) the scintillation rate and (right) the wave coherence length (this last pdf is multiplied by 10000 to match the shading scale).

Intuitively, the larger the turbulence rate along the path, the larger the scintillation rate, the lower the coherence length. Thus, on average, ρ_c is lower and S_A is larger near the surface (fig 1). Because the range-dependent weighting function is more peaked for ρ_c than for S_A, the extrema of ρ_c are in closer relation with the extrema of C_n^2. Fig 2 shows that the minima of C_n^2 decrease with height, whereas the maxima hardly change. This explains the increasing positive skewness of ρ_c with height, in contrast with the more symmetric pdf of S_A.

To better understand the variability of fig 2, let's call Lt the turnover length of C_n^2. If L<<Lt, then one realization uses a path-integration over a narrow sample of the pdf of C_n^2, so the formed diagnostic has approximately the same variability as C_n^2. If L>>Lt, then the path-averaging in eq (2) is performed over a well-sampled pdf. All propagation realizations are equivalent, and the formed diagnostic has virtually no variability. Hence, in a general sense, the variability of fig 2 decreases with L/Lt. The range L is scenario-dependent. Lt is driven by the environment, and can be assessed through the spatial organization of C_n^2.

Fig 3 shows the horizontal distribution of C_u^2 and C_T^2 at two heights, in a portion of the LES domain. The spatial organization of both fields is obvious, as well as their good correlation. The existence of vigorous updrafts is well-known in the convective boundary layer (e.g. [6]). Contoured on fig 3 is a physical threshold used to detect them, based on vertical velocity and buoyancy. In the bulk boundary layer, the updrafts explain the large excesses in C_u^2 and C_T^2. Further analysis shows that this is also true for ε_{TKE} and ε_T. Intuitively, the inner part of the updrafts is associated with large (resolved) temperature and velocity gradients in eq (6), and thus with large (parameterized) inertial-convective range fluctuations. Near the inversion, the updrafts overshoot shifts the strongest thermal gradients at the edge of the updrafts, in the entrainment-driven areas.

Fig 3 suggests that there are basically two characteristic dimensions in the distribution of C_n^2, the width of the updrafts and their interdistance. Again, this challenges the standard view of a characterization of the larger turbulent scales with a single integral (or outer) scale. Still, defining Lt as the updrafts interdistance, the LES suggests that Lt increases with height, in keeping with observations and other LES. The ratio L/Lt thus decreases, which tends to enhance the variability of S_A with height. The same tendency may exist for ρ_c, but to a lesser extent since there is less path-averaging for this diagnostic (see above).

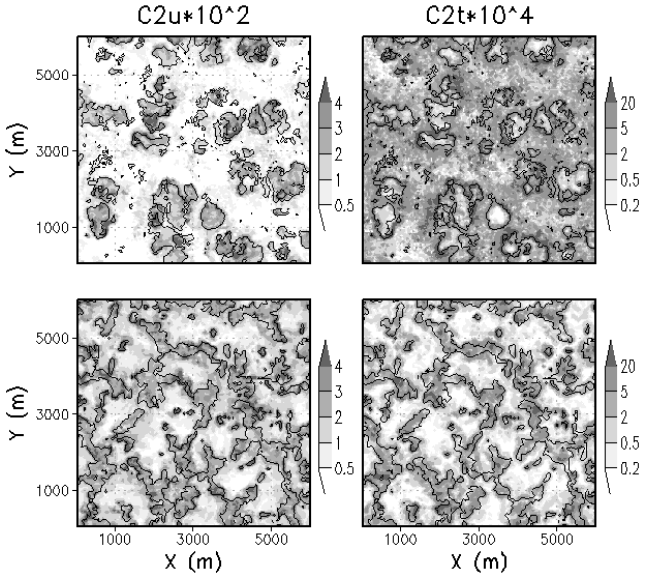

Fig 3: (x,y) cross section of C_u^2 (left) and C_T^2 (right) at Z=0.5Zi (bottom) and Z=0.95Zi (top). Contoured is the updraft threshold defined in [5].

4.2 Sound scattering

Let's now turn to the analysis of acoustical scattering. Fig 4 shows the pdf of Log(C_n^2) with the scattering angle (eq 3), as predicted from the LES at various heights. The mean behaviour is well-documented, e.g. the cancellation of the scattering at θ=90°. Again, the LES predictions stress the wide variability of C_n^2 at all scattering angles. Fig 4 also shows the contribution of temperature fluctuations to the pdf. C_T^2 is stronger in the lower boundary layer (fig 1), so the temperature fluctuations increase C_n^2 in a non negligible manner at all angles. In the bulk and upper boundary layer, the impact of C_T^2 is significant for the backward scattering only (see eq 3).

It may seem surprising that the apparently bi-modal appearance of fig 3 results in log-normal distributions (see above). To better understand this issue, fig 4 also shows the updrafts vs. environment decomposition at θ=180°. From this figure it appears that the updrafts are clearly distinct from their environment in the lower and bulk boundary layer. Hence the log-normal distribution is only an approximation of the pdf of C_u^2 and C_T^2 (and of ε_{TKE} and ε_T). These pdf can be more realistically modeled as some two-regimes distributions, one for the updrafts and the other for their environment. This conclusion is obtained by [7], based on their monostatic sodar data. The present LES data offer a comprehensive view of the underlying physics, with an assessment of the spatial organization. They suggest that a bi-static sodar would yield a comparable bi-modal distribution, including near the inversion (fig 3).

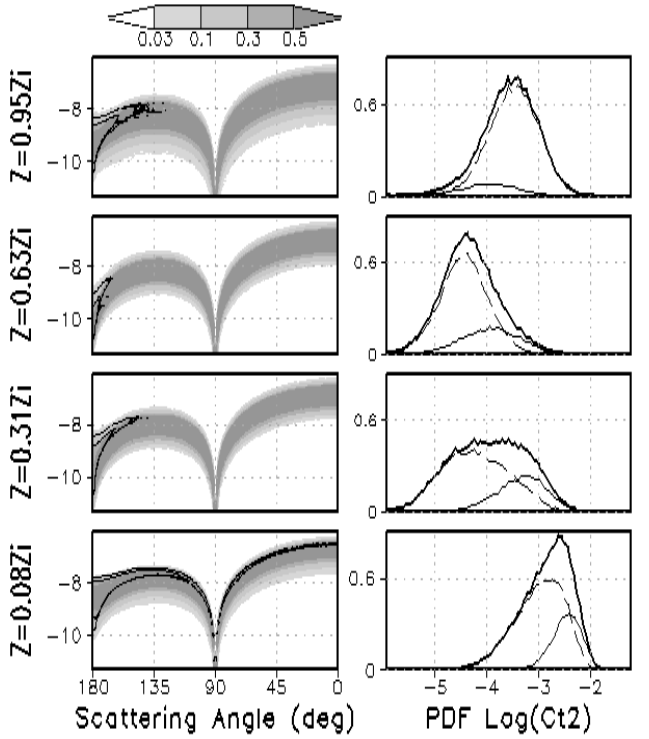

Fig 4: Left: pdf of $\mathrm{Log}(C_n^2(\theta))$ at four heights. Contours show the contribution of temperature fluctuations (eq 3). Right: pdf of $\mathrm{Log}(C_n^2(\theta=180°))$, in thick lines, with contributions from the updrafts (full lines) and the environment (dashed).

Since the scattering cross section $\sigma(\theta)$ is proportional to $C_n^2(\theta)$, it shows the same variability as in fig 4 (eq 1). To illustrate the significance of this result, consider a scenario with an acoustical source emitting in an upward refracting atmosphere. Assume that the turbulent scattering is the only (or major) contribution possibly detected by a distant surface-based sensor. Fig 4 shows that the received signal is subject to considerable variations due to the intermittency of turbulence. Characterizing the source detectability with the mean profile of C_n^2 would result in a very poor appreciation of the actual sensing performance.

Wilson et al. [8] perform a study on the subject, in the case where one contribution dominates in eq (3). They conclude that the variability of atmospheric structure parameters strongly increases the probability of measuring large values of the scattered intensity. They use a log-normal distribution of C_n^2 as model. The present LES data partially support this view (see above), and stresses the spatially-organized nature of these fluctuations. Wilson [9] further extends the analysis to the combination of wind and temperature fluctuations, based on the assumption of a joint log-normal distribution of ε_{TKE} and ε_T. A further examination of LES results shows that this assumption is deficient in the upper convective boundary layer.

Beyond the choice of a model for the pdf of the structure parameters and dissipation rates, there is a need of a physical rule to quantify the variability of these fields in the boundary layer. One metrics is the variance γ of the type of pdf shown in fig 1. Since the scattering is sensitive to the eddy size, the sensitivity of this parameter to the sampling size must also be investigated. To that purpose, the LES diagnostics are averaged over horizontal surfaces of increasing radius *r*. The results are compared to the standard inertial-convective range parameterization, here written in the form:

$$\gamma(r;z) = M(z) + \mu Ln\left(\frac{L_0}{r}\right) \tag{7}$$

where μ is a constant, and L_0, the integral scale of turbulence, is introduced for homogeneity. M(z) depends on height, it accounts for the intermittency at greater scales than L_0. The logarithmic dependence of γ in *r* is predicted by the LES for r<150m, at all heights. Fig 5 shows this dependence at Z=0.08Zi. The constant μ can be computed, with $\mu_{TKE}\approx 0.2$ (for ε_{TKE}) and $\mu_T\approx 0.5$ (for ε_T). These estimates are in good agreement with available experimental data. To our knowledge, this is the first evaluation of eq (7) based on atmospheric LES data.

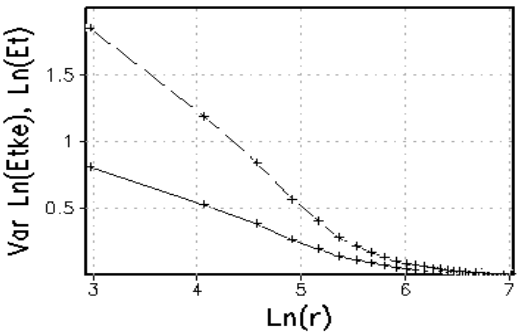

Fig 5: Variance of $\mathrm{Ln}(\varepsilon_{TKE})$ (full lines) and $\mathrm{Ln}(\varepsilon_T)$ (dashed lines) with Ln(r) at Z=0.08Zi.

The predicted value of γ for ε_{TKE} is of the order of 0.8 for radii of the order of 25m at a height of 80m, and tends to decreases with height. In comparison, Wilson et al. deduce from their acoustical measurements, performed during a convective day with a boundary layer height of 800m, that $\gamma\approx 0.7$ for ε_{TKE} in their case. The relative agreement with the LES suggests that the analysis of acoustical returns over representative periods has the potential to provide a measure of the atmospheric turbulence intermittency in the bulk boundary layer.

5 Summary and discussion

On the one hand, the small-scale turbulence is known to have dramatic impacts on acoustical wave propagation at long ranges. This sensitivity is driven by the configuration of the acoustical refractive index structure parameter, C_n^2, along the propagation path. On the other hand, it is known that this configuration depends on the large-scale turbulence. As noted in [4], the intrinsically intermittent character of the large-scale turbulence raises some relatively undocumented issues with respect to the variability of the propagated signals.

In this study, it is argued that atmospheric Large Eddy Simulations are sound to diagnose C_n^2 in the boundary layer. More precisely, one can separately estimate the wind- and temperature-related components, C_u^2 and C_T^2. The method relies on the fact that LES resolve part of the inertial-convective range. It has the same limitations as LES near very strong inversions or near the surface. Conversely, by using the inertial-convective range similarity behaviour, it circumvents the need of high resolution simulation.

The considered case study is an idealized purely convective boundary layer. The LES mean profiles of the various relevant quantities agree with the theoretical expectations,

although an underestimation is noted compared to experimental results. It is shown that C_u^2 and C_T^2 undergo a considerable horizontal variability, by almost two orders of magnitude. In the bulk boundary layer, the stronger values are driven by the buoyant ascending updrafts that drive the boundary layer dynamics. Whereas a log-normal model of the pdf of these quantities is a reasonable first-order approximation, a bi-modal distribution provides a more appropriate description of the physics at work. In that sense, the present analysis supports the results of [7].

Comparable comments hold for the related TKE and temperature variance dissipation rates. Humidity is not accounted for in the simulation. Humidity fluctuations in the convective boundary layer generally follow the updrafts vs. environment distinct behaviour, like any scalar the fluctuations of which are bottom-up driven in the convective boundary layer. Hence, one may speculate that the same comments hold for the humidity structure parameter and the humidity variance dissipation rate.

This variability of C_n^2 has some important implications on the propagated signals. On a formal point-of-view, the direct diagnostic of the configuration of C_n^2 along the propagation path makes it direct to use the analytical solutions to line-of-sight wave propagation. It is found that these solutions are applicable in the formed virtual propagation scenarii (horizontal range of 2km, frequency of 500Hz). The wave coherence length is of the order of one hundred meters. It undergoes a significant variability, which is argued to have the following sensitivities. First, at a given height, it decreases with the propagation range, due to path-averaging. Second, for a given range, it increases with height in the convective boundary layer, as the characteristic scale of atmospheric variability increases.

Again according to the standard theory of wave propagation, the ability of the turbulent atmosphere to scatter sound is directly proportional to the (local) refractive index structure parameter in the scattering volume. Thereby, the present LES results reveal that the sound scattering cross section is subject to a considerable variability at all scattering angles. This variability is expected to significantly raise the probability of measuring large sound levels when sound scattering is the dominant process. For the first time, this variability is quantified through LES data. The results confirm the validity of eq (7) in capturing the sensitivity to the size of the scattering volume. The reported intermittency parameters are of 0.2 for ε_{TKE} and 0.5 for ε_T, in agreement with available experimental data. The analysis of acoustical returns over representative periods is apparently able to provide a measure of this intermittency.

It is obvious that many of the present results may not hold in other contexts. The acoustical propagation scenario is of primary importance: propagation path (e.g. see above), wavelength, etc. The present study focuses on acoustical diagnostics which are driven by inertial-convective range turbulence. Other interesting diagnostics (e.g. angle-of-arrival fluctuations) may be more sensitive to larger turbulent scales. They might still be assessed through LES atmospheric fields, but the conclusions may be radically different from the present ones.

From the environmental side, the considered turbulence structure is specific to the convective boundary layer. Sensitivity tests show that the statistics presented in this report are rather robust with respect to the presence of a wind shear. Thus, the present conclusions may be expected to hold in boundary layer types that cover a significant portion of the globe, e.g. over warm oceans, or over continents in the daytime. It remains that many other turbulence types exist, e.g. at night-time over land (stable stratification).

Inertial-convective range turbulence is of critical concern in an extremely wide range of wave propagation applications: acoustical and optical detection, electromagnetic or acoustical remote sensing of the atmosphere, astronomy, communications, dispersion of aerosols, etc. The method and results presented in this paper may also extend to these areas, e.g. [5].

References

[1] V. Tatarski, "Wave Propagation in a Turbulent Medium", McGraw and Hill, New York (1961)

[2] D. Havelock, X. Di, G. Daigle and M. Stinson, "Spatial coherence of a sound field in a refractive shadow: comparison of simulation and experiment", *J. Acoust. Soc. Am.* 98, 2289-2302 (1995)

[3] V. Ostashev, "Sound propagation and scattering in media with random inhomogeneities of sound speed, density and medium velocity", *Waves in Random Media* 4, 403-428 (1994)

[4] M. Kallistratova, "Acoustic waves in the turbulent atmosphere: a review", *J. Atmos. Oceanic Tech.* 19, 1139-1150 (2002)

[5] S. Cheinet, P. Siebesma, "The impact of boundary layer turbulence on optical propagation", *Proc. SPIE* 6747(A), 11p (2007).

[6] S. Cheinet, "A multiple mass-flux parameterization for the surface-generated convection. Part 1: Dry plumes", *J. Atmos. Sci.,* 60, 2313-2327 (2003)

[7] I. Pentenko and E. Shurygin, "A two-regime model for the probability density function of the temperature structure parameter in the convective boundary layer", *Bound.-Layer Meteorol.* 93, 381-394 (1999)

[8] K. Wilson, J. Wyngaard and D. Havelock, "The effect of turbulent intermittency on scattering into an acoustic shadow zone", *J. Acoust. Soc. Am.* 99, 3393-3400 (1996)

[9] K. Wilson, "Scattering of acoustic waves by intermittent temperature and velocity fluctuations", *J. Acoust. Soc. Am.* 101, 2980-2982 (1997)